Molecular Phylogenetics and Evolution 53 (2009) 679–693

Contents lists available at ScienceDirect

Molecular Phylogenetics and Evolution

journal homepage: www.elsevier.com/locate/ympev

Phylogeographic analyses of the 30°S south-east Pacific biogeographic transition zone establish the occurrence of a sharp genetic discontinuity in the kelp *Lessonia nigrescens*: Vicariance or parapatry?

Florence Tellier [a,b,c], Andrés P. Meynard [a,b,c], Juan A. Correa [c], Sylvain Faugeron [c,*], Myriam Valero [a,b]

[a] UPMC Université Paris VI, UMR 7144, Equipe Evolution et Génétique des Populations Marines, LIA "DIAMS", Station Biologique de Roscoff, B.P. 74, Place Georges Teissier, 29682 Roscoff, France
[b] CNRS, UMR 7144, Equipe Evolution et Génétique des Populations Marines, LIA "DIAMS", Station Biologique de Roscoff, B.P. 74, Place Georges Teissier, 29682 Roscoff, France
[c] Departamento de Ecología and Center for Advanced Studies in Ecology and Biodiversity, LIA "DIAMS", Facultad de Ciencias Biológicas, Pontificia Universidad Católica de Chile, Casilla 114-D, Santiago, Chile

ARTICLE INFO

Article history:
Received 19 January 2009
Revised 13 July 2009
Accepted 15 July 2009
Available online 30 July 2009

Keywords:
atp8/trnS
Budding speciation
Coastal biogeographic transition
ITS
Kelp
Phylogeography
RuBisCo spacer
South-east Pacific

ABSTRACT

Phylogeographic studies are lacking in the Southern Hemisphere, and in particular in the south-eastern Pacific. To infer the possible scenario for the debated biogeographic transition zone located at 30–33°S along the Chilean coast, we investigated whether there is a concordance between the phylogeographic pattern and the biogeographic transition in the intertidal kelp *Lessonia nigrescens* whose distribution is continuous across this transition zone. Using a combination of four makers located in the three genomic compartments (chloroplast, mitochondria and nucleus), we showed the presence of two main divergent lineages, possibly cryptic species. There was an exact match of the phylogeographic break with the 30°S biogeographic transition zone, suggesting a common origin. The combined information given by the multilocus approach and by the population analysis suggested the occurrence of a budding speciation, with a northward range expansion.

1. Introduction

In the current context of global change, it has become of primary interest to understand the processes affecting a species' range as well as the factors influencing speciation processes. The distribution of species is the result of both historical and contemporary processes that often lead to similar patterns of distribution among species separated by biogeographic transition zones. The role of demographic history versus selection for creating these patterns has always puzzled evolutionists and the debate about sympatric and allopatric speciation remains controversial (Bolnick and Fitzpatrick, 2007; Fitzpatrick et al., 2008). Phylogeography, the study of the geographic distribution of gene lineages within species, allows us to understand the evolution of diversity. It is used, in particular, to test for the congruence between patterns of geographic boundaries, such as a biogeographic transition zone, and genetic discontinuities for species whose distribution cross those transition zones (Avise, 2000). Theoretical expectations are, however, not straightforwardly met by genetic data because genetic discontinuities can arise from a number of factors that include variable levels of selection, drift and gene flow. For instance, for species showing restricted dispersal capacities, local genetic drift can promote the emergence of highly differentiated clades that are geographically separated even in the absence of any physical or ecological barrier to dispersal (Irwin, 2002). In addition, the recent work of Hallatschek et al. (2007) proved experimentally that the neutral process of genetic drift combined with demographic expansion can also lead to a strong spatial structure of genetic diversity. Consideration of the stochastic nature of genetic processes through the implementation of the coalescent theory and the development of statistical phylogeography (Knowles, 2004) allows in-depth analyses and tests of the possible scenarios that can be inferred from a particular set of genetic patterns of distribution.

Coastal marine biogeographic transition zones have been described in all oceans and the concordance with phylogeographic breaks has been shown for a great variety of organisms (e.g. north-eastern American coast: Avise, 2000; north-western American

* Corresponding author. Fax: +56 23 54 26 21.
E-mail address: sfaugeron@bio.puc.cl (S. Faugeron).

1055-7903/$ - see front matter © 2009 Elsevier Inc. All rights reserved.
doi:10.1016/j.ympev.2009.07.030

coast: Dawson, 2001; south-eastern Australian coast: Dawson, 2005; northern Atlantic: Maggs et al., 2008). These genetic discontinuities generally result from cyclical variations in sea level and surface temperatures that occurred during the Pleistocene glacial episodes which caused extended and important changes in coastal topology, creating effective barriers to dispersal. These past physical barriers resulted in vicariant processes that are easily detectable by phylogeographic analyses, in particular for species characterized by a short dispersal distance. Other known biogeographic transitions are associated with oceanographic conditions that create present day barriers to dispersal, i.e. Point Conception where the southward cool California current veers offshore whereas a warmer eddy flows up the coast from the south, warming the southern California coast (Wares et al., 2001), or the confrontation of the southwestward tropical Agulhas current with the northwestward upwelling Benguela current in South Africa (von der Heyden et al., 2008).

Along the Chilean coast (18°S–56°S), three biogeographic regions are recognized (Camus, 2001; Thiel et al., 2007): (1) the Peruvian Province (PP) includes warm-temperate biota and ranges from Peru to 30°S, (2) the Magellanic Province (MP) with a sub-Antarctic cold-temperate biota extending from 40–42°S to 56°S, and (3) the Intermediate Area (IA), made of mixed components of the two former Provinces, extends from 30°S to 40–42°S. The significance of the 30°S transition zone is, however, still controversial as it is not observed for all taxa and its geographic location is less clear (between 30 and 33°S) and varies depending on the authors and the taxa (reviewed by Camus, 2001 and Thiel et al., 2007). One of the unanswered questions regarding the 30°S biogeographic transition is whether it is the result of current ecological conditions, as evidenced by changes in recruitment patterns of mussels and barnacles around 32–33°S (Navarrete et al., 2005; Broitman et al., 2001), or it has an ancient origin, linked to either major ecological changes or to some physical barriers that no longer exist. Present day coastal oceanographic features, such as strong kinetic eddies present at 30°S (Hormazabal et al., 2004), are likely to effectively limit dispersal around 30°S. Such an effect has been shown for Cape Blanco (42°N) in Oregon (Connolly et al., 2001), a region affected by similar shifts in upwelling regimes favoring strong reduction in recruitment and genetic clines in invertebrate species (Sotka et al., 2004). Such ecological limitations to dispersal are likely to contribute to the maintenance of the biogeographic transition. However, a vast number of plastic or long dispersal species have a distribution that crosses 30°S without any apparent change in density (Broitman et al., 2001). Indeed, it has been shown for the gastropod *Concholepas concholepas*, a species present from Cape Horn to Northern Peru and characterized by an particularly high dispersal potential, that the 30°S region does not represent any effective barrier to dispersal neither in the present nor in the past, as indicated by a total absence of genetic structure (Cárdenas et al., 2009). Considering the above, we investigated whether there is a concordance between the phylogeographic pattern and the biogeographic transition in a species characterized by short distance dispersal, the intertidal kelp *Lessonia nigrescens* (Faugeron et al., 2005; Martínez et al., 2003). The distribution of this kelp ranges from 17°S (Peru) to 56°S (Cape Horn) (Searles, 1978) and therefore covers the three major biogeographic units described along the Chilean coast. The wide range of latitudinal distribution of this species makes it a good model to test for the hypothesis of a genetic continuity across the 30°S transition zone. On the other hand, its limited dispersal capacity should make it particularly sensitive to processes such as vicariance or founder effects.

In order to properly infer the processes likely shaping the phylogeographic structure, we first used a combination of four different markers characterized by different mutation rates and different effective sizes: the recently developed mitochondrial marker atp8/trnS (Engel et al., 2008), the chloroplastic RuBisCo spacer, and the nuclear rDNA Internal Transcribed Spacers, ITS1 and ITS2. As a consequence of the difference in ploidy level and the generally uniparental inheritance pattern, mitochondrial and chloroplastic markers are characterized by a reduced effective size and are therefore more susceptible to be affected by genetic drift than nuclear markers (Ballard and Rand, 2005). Cytoplasmic markers are thus more likely than nuclear ones to show a pronounced phylogeographic structure, either of deterministic origin (i.e. caused by an historical barrier to gene flow) or of stochastic origin (i.e. caused haphazardly by the genetic drift) (Irwin, 2002; Kuo and Avise, 2005). Furthermore ITS2 and RuBisCo spacer are generally considered to have lower mutation rates than ITS1 and mitochondrial markers (e.g. for brown algae: Coyer et al., 2001; Yoon and Boo, 1999; Harvey and Goff, 2006; Engel et al., 2008), potentially enabling the detection of different processes occurring at different time scales. Finally, it has been shown that using a single locus to infer the phylogeographic structure of a species can be misleading because of the potential consequences of the selective processes on mitochondrial DNA, such as selective sweeps and background selection, in shaping intraspecific diversity (Ballard and Whitlock, 2004; Bazin et al., 2006). Comparison of these diverse and independent markers from different genomic regions facilitates the distinction of the different processes (selection, drift and history) when interpreting the phylogeographic structure. Furthermore, we also aimed to investigate further the processes acting both around the 30°S transition and within each biogeographic region. In addition to the multilocus approach, we developed a population genetics analysis based on the mitochondrial marker, in order to determine accurately the geographic distribution of lineages and to assess the variability within populations.

2. Materials and methods

2.1. Model species

The genus *Lessonia* is defined by Santelices and Meneses (2000) as a sub-Antarctic component of the marine flora whose distribution includes (besides the Chilean and Peruvian coast) New Zealand, sub-Antarctic islands, and Tasmania. As with all the Laminariales, *L. nigrescens* has a heteromorphic haploid–diploid life cycle in which the diploid sporophyte is the macrophyte (up to 4 m long) and the haploid phase is a dioecious microscopic filament. The encounter of gametes is likely under the control of pheromones (Lünning and Müller, 1978) and fertilization occurs on the female gametophytes. Dispersal is thought to be achieved mainly by haploid spores emerging after meiosis from the sporophyte, although some long-distance dispersal events may occur (Faugeron et al., 2005). However, these motile spores have a short lifespan, with a limited capacity to adhere to the substratum (less than 24 h, Martínez, com. pers.), thus limiting the dispersal capacity of the species.

2.2. Sampling

For the multilocus approach, a total of 127 individuals of *L. nigrescens* was sampled in 36 rocky intertidal locations, with 2–6 individuals collected per location (Table 1, Supplementary material-Fig. S1) ranging from 17°37′S (Peru) to 41°38′S (Chiloé Island, Chile), thereby covering 3/4th of the known species distribution range (Searles, 1978). A more intensive sampling was done between 27°S and 34°S, in an effort to examine with higher resolution the biogeographic transition zone. Samples of *L. trabeculata* (eight individuals), *L. flavicans* (two individuals) and *L. vadosa*

Table 1
Geographical location of the sampled sites. *N*, number of individuals analyzed per site and for each marker; N_{TOTAL}, total number of individuals analyzed per site for the atp8/trnS population-level analysis; N_{SEQ}, number of samples analyzed by sequencing; N_{SSCP}, number of samples analyzed by SSCP.

Sampled sites	Abbreviation	Coordinates (latitude/longitude)	*N* atp8/trnS	*N* RuBisCo spacer	*N* ITS1	*N* ITS2	Population analyse (atp8/trnS)		
							N_{TOTAL}	N_{SEQ}	N_{SSCP}
L. nigrescens									
Qda Mollendito-Perú	QMO	16°58′S/72°07′W	0	0	0	0	30	2	30
Ilo-Perú	ILO	17°37′S/71°20′W	5	5	1	2	0	—	—
Qda Camarones	CAC	19°11′S/70°16′W	4	2	0	2	30	2	30
Pta Pichidalo	PCH	19°36′S/70°14′W	2	2	2	2	29	3	27
Pta Patache	PAT	20°48′S/70°12′W	2	2	0	0	28	3	26
Pta Coloso	COL	23°46′S/70°29′W	5	5	0	1	30	5	30
Pan de Azúcar	SLD	26°09′S/70°40′W	5	5	2	1	29	2	28
Morro Copiapó	MOC	27°12′S/70°57′W	5	5	2	1	30	5	30
Cta Pajonal	PAJ	27°41′S/71°02′W	3	3	2	2	30	3	30
Carrizal Bajo	CAR	28°04′S/71°08′W	5	5	2	3	30	5	30
Huasco	HCO	28°27′S/71°13′W	5	5	2	2	8	5	8
Aceituno	ACE	29°03′S/71°29′W	5	5	1	2	29	29	0
Choros Norte	CHN	29°15′S/71°27′W	2	2	2	2	30	2	30
Choros Sur	CHS	29°21′S/71°19′W	5	5	3	3	30	5	30
El Temblador	TBL	29°28′S/71°18′W	2	2	0	0	33	2	33
Isla Pájaros (Island)	IPA	29°35′S/71°31′W	5	5	2	2	30	30	0
Arrayan	ARY	29°41′S/71°19′W	2	2	1	2	33	3	33
Teatinos	TEA	29°49′S/71°17′W	5	5	1	2	30	5	30
Coquimbo-Cruz	COZ	29°57′S/71°21′W	5	5	1	2	28	28	0
Totoralillo	OTO	30°04′S/71°22′W	4	4	1	2	30	5	30
Guanaqueros	GUANA	30°11′S/71°27′W	2	2	2	2	32	3	32
Tongoy	TON	30°14′S/71°29′W	2	2	2	2	30	2	30
Pta Lengua de Vaca 2	PTLV2	30°15′S/71°38′W	4	4	1	2	30	30	0
Cta San Lorenzo	CSLO	30°20′S/71°40′W	2	2	0	2	0	6	—
Río Limari	RLI	30°44′S/71°42′W	3	2	2	3	29	29	0
Pta Talca	PTAL	30°55′S/71°40′W	5	5	2	2	31	8	31
Los Molles	LM	32°14′S/71°31′W	2	2	1	2	33	2	33
Montemar	MTM	32°57′S/71°32′W	2	2	2	2	33	12	33
Curaumilla	CURAM	33°05′S/71°43′W	5	5	2	2	30	16	30
El Quisco	QUIS	33°23′S/71°42′W	2	2	2	2	30	18	14
Las Cruces	LC	33°30′S/71°38′W	2	2	2	2	30	16	27
Matanzas	MAT	33°57′S/71°52′W	2	2	1	2	30	8	25
Pichilemu	PICHI	34°23′S/72°01′W	0	0	0	0	30	19	14
Constitución	CST	35°19′S/72°25′W	2	2	0	0	12	12	0
Concepción	CONCE	36°30′S/72°54′W	5	5	2	2	28	27	5
Mehuin	MEH	39°25′S/73°12′W	5	5	2	2	30	30	0
Pucatrihue	PUC	40°32′S/73°43′W	2	2	2	2	30	30	0
Pta Guabún (Chiloé Island)	GBN	41°48′S/74°01′W	4	4	2	2	30	30	0
Total *L. nigrescens*	38 locations		127	124	52	66	1045	434	729
L. trabeculata									
Trompa del elefante—Perú	Lt-TRU	15°23′S/75°09′W	1	1	1	1			
Cabañas	Lt-CAB	20°18′S/70°08′W	1	1	1	1			
Huasco	Lt-HCO	28°27′S/71°13′W	1	1	1	1			
Tongoy	Lt-TOY	30°14′S/71°29′W	1	1	0	1			
Algarrobo	Lt-ALGA	33°21′S/71°40′W	1	1	1	1			
Pta Estaquilla	Lt-EST	41°23′S/73°44′W	1	1	1	1			
Ancud (Chiloé Island)	Lt-ANC	41°48′S/74°01′W	2	1	1	1			
Total *L. trabeculata*	7 locations		8	7	6	7			
L. flavicans									
Fuerte Bulnes	Lfla-FBA	53°35′S/73°41′W	1	1	1	1			
Isla Elisa	Lfla-ELI	54°19′S/71°37′W	1	1	1	1			
Falkland Islands, UK		51°43′S/57°54′W	0	1[a]	1[a]	1[a]			
L. vadosa									
Fuerte Bulnes	Lvad-FBA	53°35′S/73°41′W	1	1	1	1			
L. corrugata									
Tasmania		41°52′S/148°18′E	0	1[b]	1[b]	1[b]			

Data from GenBank (from Lane et al., 2006).
[a] *L. flavicans*: Accession Nos. AY851543 (RuBisCo spacer) and AY857900 (ITSs).
[b] *L. corrugata*: Accession Nos. AY851545 (RuBisCo spacer) and AY857902 (ITSs).

(one individual) were also collected (Table 1). The first species is present from 12°S (Peru) to 41°S (Chiloé Island), whereas the two other species are restricted to the southern tip of South America (47–56°S). All these latter species are subtidal.

In order to infer the structure within lineages and within populations, an additional sampling of 28–33 individuals per location (with the exception of HCO: 8 individuals, and CST: 12 individuals) was done in 36 locations (Table 1). Individuals were sampled by collecting fragments of frond along a 100–150 m transect. Each sample consisted of cleaned basal fragments of fronds excised from fresh thalli and immediately placed into a plastic bag filled with silica gel beads for rapid dehydration.

2.3. DNA extraction and sequencing for the multilocus approach

Dried material was grounded in liquid nitrogen, and 50 μL of tissue powder was used for DNA extraction. The extraction procedure combined a standard Cetyltrimethyl Ammonium Bromide (CTAB) extraction with the addition of Polyvinyl Pyrolidone (PVP) to extract polyphenols (Martínez et al., 2003). The precipitated DNA pellet was diluted in 60 μL of MilliQ water and quantified by NanoDrop (NanoDrop Technologies Wilmington, Delaware, USA).

One to five individuals per location were analyzed using the four markers atp8/trnS, RuBisCo spacer, ITS1 and ITS2. The mitochondrial marker atp8/trnS was amplified with the primers developed by Engel et al. (2008); using the PCR and program from Voisin et al. (2005). The plastid marker RuBisCo spacer, developed first in algae by Destombe and Douglas (1991), is composed of the RuBisCo spacer and part of the sequences coding for the large and for the small subunits of RuBisCo. The amplification of this plastid region was done using the primers RS1 and RS2 designed by Yoon and Boo (1999). Primers LB1 and LB2 (Yoon et al., 2001) were used to amplify ITS1 and ITS2. For the RuBisCo spacer and the ITS markers, reaction mix followed the same protocols, with the exception of the bovine serum albumin (0.3 mL mL^{-1}) and PCR conditions were adapted from Yoon and Boo (1999) with some modifications (30 cycles, elongation for 45 s at 57 °C for ITSs and at 50 °C for RuBisCo spacer). PCR products were purified and sequenced on an ABI PRISM® 3100 Automated DNA Sequencer (Applied Biosystems, Foster city, CA, USA).

Due to some sequencing difficulties, polymorphism within some individuals was suspected for ITS markers. These sequences were discarded from the data set. However, DNA from five individuals from the 30°S biogeographic transition zone that showed polymorphism (SLDN6, CAR1, TBL2, PTLV2–11, PTAL3) were cloned in order to detect whether this within-individual polymorphism could be explained by hybridization between entities located on both sides of the 30°S biogeographic transition. The PCR products were cloned using the pGEM®-T Vector System (Promega, Madison, WI, USA) following the manufacturer's protocol. Up to five clones were sequenced per individual.

2.4. SSCP and sequencing for the population-level study

To investigate the polymorphism of the atp8/trnS marker at the population-level, we completed the previous data set obtained by the sequencing method with the rapid screening method of single-strand conformation polymorphism (SSCP) (Orita et al., 1989; Sunnucks et al., 2000). Using the same PCR as previously described, PCR products were loaded in non-denaturing polyacrylamide gels in order to identify mutations affecting the conformation of single-strand DNA. About 16 μL of PCR product were mixed with 32 μL of denaturing/loading buffer containing 8 μL of 15% ficoll loading buffer (with 0.25% bromophenol blue and 0.25% xylene cyanol), 5 μL urea 5 M and 19.7 μL TBE 1× buffer. After denaturating 4 min at 94 °C, amplification products were separated using 10% polyacrylamide (37.5:1 acrylamide:bisacrylamide) gels run in 0.5× TBE at 200 V during 17 h at 4 °C on a vertical electrophoresis system (Bio-Rad, Hercules, CA, USA). After electrophoresis, SSCP gels were stained for 20 min with a 2.5× Sybr Gold solution and bands were visualized under UV light.

Previously sequenced haplotypes were used as profile references in each SSCP gel. To check for the consistency of the SSCP typing, we sequenced at least two individuals for each different SSCP profile and for each location whenever possible. For profiles corresponding to more than one haplotype, we did an additional screening by RFLP using the restriction enzymes DraI and AseI. Discrimination of the different restriction profiles was done by migration on 12% acrylamide gels.

2.5. Sequences alignment and polymorphism of the four markers

Sequences were edited using Chromas (McCarthy, 1997) and multiple sequence alignments were constructed with Multalin (Corpet, 1988). Sequences from GenBank of another *L. flavicans* individual from Falkland Islands and of an individual of *Lessonia corrugata* (only present in Tasmania) were included (Table 1). Only the spacer region was considered for ITS1 and ITS2 analyses. For atp8/trnS, we considered 13 bp of the 3′ end of the *atp8* gene, the *atp8/trnS* intergenic region and 23 bp of the 5′ end of the *trnS* gene. The RuBisCo spacer alignment consisted of 198 bp of the 3′ end of the *rbcL*, the RuBisCo spacer, and 121 bp of the 5′ end of the *rbcS*. For each marker we computed the number of polymorphic sites (s) considering only nucleotide substitution and the gene diversity index (H), based on allele frequency (Nei, 1987), using Arlequin v 3.11 software (Excoffier et al., 2005).

2.6. Phylogenetic analyses for the multilocus data sets

Indels in the ITS and RuBisCo spacers data sets did not provide any phylogenetic information and were treated as missing data. In contrast, indels were informative for the atp8/trnS data set and thus were treated using three methods: considering indel sites as missing data, excluding indel sites and coding indels as present or absent. The automated coding of indels was implemented using the "IndelCoder" menu available in SeqState (Müller, 2006). We applied the Simple Indel Coding (SIC), a method that considers stretches of indel sites as non-independent characters and treats each indel as a separate binary character (Simmons and Ochoterena, 2000). The ITS1 and ITS2 sequences were treated independently because each may evolve at different rates (Hershkovitz and Lewis, 1996) and phylogenetic analyses of these markers were done with and without cloned sequences. Trees were rooted with either *L. corrugata* or *L. vadosa* as outgroup, except for atp8/trnS analyses for which no sequence from *L. corrugata* was available.

The different alignments were analyzed using maximum parsimony (MP) and maximum likelihood (ML) methods using PAUP* v 4.0b10 (Swofford, 2002) and Bayesian inference (BI) using MrBayes v 3.1.2 (Huelsenbeck and Ronquist, 2001). Under parsimony, heuristic searches included 100 random addition sequence replicates, tree-bisection-and-reconnection (TBR) option for branch swapping and the maximum number of trees was fixed to 100,000. Nodal support was assessed using non-parametric bootstrap (Felsenstein, 1985) with 1000 pseudo-replicates using a heuristic search with the TBR option for branch swapping. For each marker, we used the Akaike Information Criterion (AIC) implemented in ModelTest v 3.7 (Posada and Crandall, 1998) to estimate the best fit model parameters for the ML reconstruction method. The selected models were K81uf+I for the RuBisCo spacer and the atp8/trnS data sets, TnEf+I for the ITS1 data and HKY for the ITS2 data. ML analyses were performed with heuristic searches with 100 random sequence addition replicates and nodal support was assessed using non-parametric bootstrap analyses with 1000 pseudo-replicates. Bayesian inference was performed using the general type of the best fit model parameters defined for each data set, in which four independent analyses were run with four chains each, for five million generations. Trees and parameters were sampled every 1000 generations and the default parameters were used to fit temperature and swapping. The first 25% of sampled trees were discarded to ensure stabilization and the remaining used to compute a consensus tree. The split frequency (variance between the four independent runs) in all cases was below 0.005, confirming that sampling was from the posterior probability distribution. In

the case of the atp8/trnS partition in which indels were coded with the SIC method, the mixed matrix obtained with IndelCoder was used as an input file in MrBayes. Here the nucleotide sequences were analyzed with the selected model, whereas the matrix of presence/absence of indels was treated as restriction site data.

2.7. Sequences divergence and estimation of divergence time

The sequence divergence between the different sets of sequences grouped according to their phylogenetic affinities (i.e. lineages) was obtained as uncorrected *p*-distances (i.e. the proportion *p* of nucleotide sites at which two compared sequences are different) calculated with MEGA v 4.0 (Kumar et al., 2004), with 1000 replicates excluding indels from data analyses.

The rate of molecular evolution was estimated following Hoarau et al. (2007), who estimated the mutation rate for the photosystem II chloroplast protein D1 (*psbA*) between 0.08% and 0.12% per million years (Myr), based on diatoms fossil record. Given the sequence divergence for *psbA* gene (1.2%) between the two Laminariales species, *Laminaria digitata* (AY528849) and *Alaria crassifolia* (AY528847), their divergence time was estimated to be 10–15 Myr BP (1.2/0.12 and 1.2/0.08, respectively). These two species showed 8% divergence for the RuBisCo spacer (sequences AY851559 and AF109802, only the region used for *L. nigrescens* was considered). The divergence rate for RuBisCo spacer was therefore estimated between 0.53 and 0.80%.Myr^{-1} (8/15 and 8/10, respectively). Generation time effects could be neglected in our calculations since they were equivalent between diatoms, *L. digitata* and *L. nigrescens*, that is from one to few years (Hoarau et al., 2007; Chapman, 1993; Faugeron, pers. obs.). We could verify that this estimate of the molecular clock was relatively insensitive to the selected *Lessonia* species or haplotype within species (data not shown). The divergence time between the different *Lessonia* lineages was then estimated as a range between minimum and maximum coalescent times between haplotypes with MEGA v 4.0 (Kumar et al., 2004), with 1000 replicates excluding indels from data analyses.

2.8. Network reconstructions

As they assume bifurcating trees, traditional phylogenetic methods may not be appropriate for inferring intraspecific phylogenetic relationships. The representation of ancestral haplotypes as occupying branches of zero-length at the basal node of a cluster relies, therefore, on an inappropriate model (Posada and Crandall, 2001). In contrast, network reconstructions are more appropriate at the intraspecific level and particularly they specifically incorporate the possibility for the persistence of ancestral haplotypes in the data. We therefore constructed haplotypes networks using the median-joining method implemented in NETWORK v 4.5 (Bandelt et al., 1999).

2.9. Analyses of the population-level study

Molecular diversity indices as gene diversity (*H*, the probability that two randomly chosen haplotypes/ribotypes are different) and nucleotide diversity (π, the probability that two randomly chosen homologous nucleotide sites are different) were calculated for each sampled locations and for each phylogenetic lineage using Arlequin v 3.11 (Excoffier et al., 2005). The number of polymorphic locations and the mean *H* and π over locations were also calculated excluding the two locations with less than 28 individuals, i.e. Huasco (HCO) and Constitución (CST).

To test for the occurrence of genetic divergence on both sides of the transition zone, populations were grouped according to their geographic location. As the precise location of the biogeographic transition zone remains controversial among authors (between 30°S and 33°S), we tested for a discontinuity both at 30°S and at 33°S. A hierarchical analysis of molecular variance (AMOVA) was implemented in Arlequin v 3.11 (Excoffier et al., 2005) to analyze the partition of genetic variance among and within these geographic regions. The φ-statistics were calculated as pairwise differences among locations and their significance was computed using a non-parametric permutation test with 10,000 permutations.

Isolation by distance (Slatkin, 1993) was tested by plotting pairwise genetic distances against pairwise geographical distances using Mantel test implemented in Arlequin v 3.11 (Excoffier et al., 2005; 1000 permutations and excluding HCO and CST). To compute a linear relationship, genetic distances were measured as $\pi/(1-\pi)$, where π is the mean pairwise difference among locations following the recommendations of Rousset (1997). Geographical distances were measured as distances along the coast for continental locations and taken as the straight-line distance for the island Isla Pájaros (IPA) and Pta Guabun (Chiloé Island, GBN) locations.

Mismatch distribution analyses were done for each phylogenetic lineage using Arlequin v 3.11 to infer demographic history. Both sudden demographic expansion (Rogers and Harpending, 1992) and spatial expansion (Excoffier, 2004) models were fitted to the observed mismatch distribution and tested using 1000 bootstraps.

A median-joining network of haplotypes was constructed for the complete atp8/trnS data set using NETWORK v 4.5 (Bandelt et al., 1999).

3. Results

3.1. Multilocus approach: polymorphism of the four markers

The principal characteristics of the four markers are given in Table 2. The length of the alignments was 159 bp for atp8/trnS (GenBank Accession Nos. EU652976–EU652987, FJ410103–FJ410116, FJ410128 and FJ410130), 349 bp for ITS1 (GenBank Accession Nos. FJ410031–FJ410059), 237 bp for ITS2 (GenBank Accession Nos. FJ410068–FJ410083) and 555 bp for the RuBisCo spacer (GenBank Accession Nos. FJ410085–FJ410102, see also Supplementary material for details). The alignments of all markers required the introduction of indels, of 1–46 bp, leading to important variation in sequence length within and between species (Table 2). Two classes of markers could be distinguished based on their polymorphism patterns within *L. nigrescens*: the atp8/trnS and ITS1 markers presented 22 haplotypes and 24 ribotypes respectively, whereas 13 ribotypes and 13 haplotypes were recovered for ITS2 and RuBisCo spacer (Table 2). The proportion of polymorphic sites was also higher in atp8/trnS and ITS1 (18% and 10%) than in ITS2 and RuBisCo spacer (6% and 2%). Most of the atp8/trnS and ITS1 alleles (i.e. either haplotypes or ribotypes) presented a geographically restricted distribution, whereas some ITS2 alleles showed a wide geographic distribution, such as the southern its2-11 allele (from IPA to GBN, 1680 km) and the northern its2-1 allele (from ILO to MOC, 1300 km) (Supplementary material-Fig. S1, for details of the geographic distribution of alleles, see also Supplementary material). Likewise, RuBisCo spacer haplotypes were shared among populations geographically distant, such as the southern haplotype rs7 (from IPA to GBN, 1680 km) or the northern haplotype rs1 (from ILO to COL, 850 km) (Supplementary material-Fig. S1). Whatever the marker used, no allele was shared between the northernmost and the southernmost locations.

Depending on the marker, the size and polymorphism of indels were highly variable. The ITS1 alignment required the insertion of 53 bp (indels of 1–14 bp length), of which 16 bp were needed for

Table 2
Characteristics of the markers used for the multilocus approach. No ind, number of individuals; No alleles, number of alleles; *bp*, the length in base pairs of the sequenced region; *s*, number of polymorphic sites for substitution; *Indels*, number of polymorphic sites for indels; *H*, within-group mean gene diversity. Groups were defined with reference to the three atp8/trnS clades (Northern, Z30 and IA) and with reference to the two ITS1 clades (PP and IA).

	No ind	No alleles	*bp*	*s*	*Indels*	*H*
atp8/trnS						
PP	65	11	155	19	27	0.888 ± 0.014
Northern	28	5	155	6	0	0.730 ± 0.047
Z30	37	6	136	5	8	0.806 ± 0.032
IA	62	11	120	11	0	0.863 ± 0.025
Lnig	127	22	155	28	37	0.938 ± 0.007
All	138	27	159	42	46	0.946 ± 0.006
RuBisCo spacer						
PP	63	6	555	5	0	0.785 ± 0.022
Northern	26	3	555	2	0	0.569 ± 0.083
Z30	37	3	555	3	0	0.581 ± 0.042
IA	61	7	555	5	1	0.727 ± 0.048
Lnig	124	13	555	11	1	0.879 ± 0.013
All	136	21	555	24	7	0.899 ± 0.012
ITS1						
PP	25	14	330	20	10	0.940 ± 0.025
Northern	7	5	330	8	9	0.904 ± 0.103
Z30	18	9	325	13	3	0.895 ± 0.043
IA	27	10	329	11	6	0.874 ± 0.040
Lnig	52	24	336	34	16	0.953 ± 0.013
All	63	32	349	52	53	0.966 ± 0.009
ITS2						
PP	31	8	231	10	2	0.851 ± 0.028
Northern	9	2	229	5	0	0.222 ± 0.166
Z30	22	6	231	5	2	0.822 ± 0.037
IA	35	5	231	4	2	0.400 ± 0.100
Lnig	66	13	233	15	6	0.801 ± 0.041
All	78	19	237	28	11	0.854 ± 0.032

PP: Peruvian Province (composed of the Northern and Z30 groups); IA: Intermediate Area; *Lnig*: *L. nigrescens* (composed of the PP and IA groups); All: all samples studied, including outgroup species.

the *L. nigrescens* alleles only (Table 2). The insertion of 11 bp and 7 bp was necessary for the ITS2 and the RuBisCo spacer alignments respectively (Table 2). The atp8/trnS marker presented a distinct pattern in terms of indels distribution, as most of the indels were included in the *L. nigrescens*-only alignment (37 of 46 bp). A polymorphism of indels was observed in two distinct regions of the atp8/trnS sequence (region 1: from 50 to 80 bp position and region 2: from 122 to 127 bp position, Fig. 1). The first indel region exhibited both a polymorphism in length and substitutions (three different indel lengths: 13, 21 and 29 bp were recognized, Fig. 1) whereas the second indel region was 6 bp long and did not present any length polymorphism.

3.2. Lessonia nigrescens divided into two main lineages

The phylogenetic reconstructions were congruent among markers to confirm that *L. nigrescens* forms a monophyletic group, with *L. trabeculata* being the closest outgroup species. The monophyly of *L. nigrescens* was consistently supported by high bootstrap and posterior probability values regardless the marker and the method for phylogenetic reconstruction (Fig. 2 for atp8/trnS and ITS1 & Fig. 3 for RuBisCo spacer and ITS2). In addition, two distinct groups of alleles were retrieved: a northern group corresponding to the Peruvian Province region ranging from 17°37′S to 30°14′S (PP lineage) and a southern group corresponding to the Intermediate Area region ranging from 29°03′S to 41°48′S (IA lineage). Support values for the PP lineage showed variation depending on the marker and on the phylogenetic reconstruction method used (Figs. 2 and 3). While the PP lineage was always monophyletic regardless of the marker, the monophyly of the IA lineage was observed only with atp8/trnS and ITS1 (Fig. 2). ITS2 and RuBisCo spacer markers presented a similar pattern, with a PP lineage supported by weak statistical support and, more generally, weak support values within the *L. nigrescens* clade and a polytomy for the IA alleles (Fig. 3). These two phylogenetic trees suggested incomplete lineage sorting due to the presence of ancestral alleles within the data set, with the presence of zero-length branches. This was confirmed by the structure of the ribotype and haplotype networks which showed a separation between alleles in individuals from the PP lineage and those encountered in the IA lineage (Fig. 3). Haplotype rs7 and ribotype its2-11 were considered as ancestral according to their position on the phylogenetic trees (zero-branch length from the nodes) and on their central position in the networks, and also because they were the most frequent and most widely distributed alleles. These ancestral alleles for both markers were observed in the IA lineage only (Fig. 3).

In addition to the IA lineage, the atp8/trnS marker showed a supplementary sub-division of the PP lineage into a "Northern clade" and a "30°S Zone clade" (Z30 clade) with high support values for each of the three clades (71–100%, Fig. 2). These two last clades presented disjoint distribution ranges: the Northern clade was observed north from 27°S whereas the Z30 clade was restricted to a narrower region between 27°S and 30°S (Supplementary material-Fig. S1, see also population-level analysis). Such a sub-division of the PP lineage in two clades was not detected for any of the other three markers, although no allele was found shared between these two sub-regions (Z30 and north from 27°S, Figs. 2 and 3).

When indel polymorphism information was used alone, four groups of atp8/trnS haplotypes could be distinguished which corresponded to the three clades previously described, with the Z30 clade grouping two different indel lengths haplotypes (first indel of 13 and 21 bp, Fig. 1). The inclusion of recoded indels in the data analyses did not modify the topology of the MP and Bayesian trees for atp8/trnS marker, except that branch lengths were consistently longer than when excluding them or treating them as missing data (data not shown). Because indel recoding is generally considered less parsimonious than indel exclusion, we chose to show only ML trees with indels treated as missing data for comparisons among the four study markers (Figs. 2 and 3).

The occurrence of within-individual polymorphism, with up to three different sequences per individual, was detected between ITS clones. Several of these sequenced clones corresponded to sequences absent of the dataset obtained by direct sequencing (GenBank Accession Nos. FJ410060–FJ410067 and FJ410084). However, each individual contained alleles either from the PP or the IA lineage, but never from both lineages, indicating that the within-individuals' polymorphism was not the result of hybridization. Moreover, the addition of the sequenced clones in the data set did not modify the topology of the phylogenetic trees (data not shown).

For ITS1 and ITS2 markers, the diversity in terms of number of alleles, number of polymorphic sites (*s*) and gene diversity (*H*), was generally higher for the PP lineage than for the IA lineage (Table 2). For instance, the most polymorphic marker, ITS1, had almost twice substitutions sites in PP ($s = 20$) than in IA ($s = 11$). The atp8/trnS marker showed exactly the same number of haplotypes in the PP and IA lineages for the multilocus data set, whereas the number of polymorphic sites observed within PP doubled those within IA (Table 2).

3.3. Sequence divergence among Lessonia nigrescens lineages and divergence timing

When sequence divergence was calculated for markers showing monophyletic clades, the divergence between lineages PP and IA

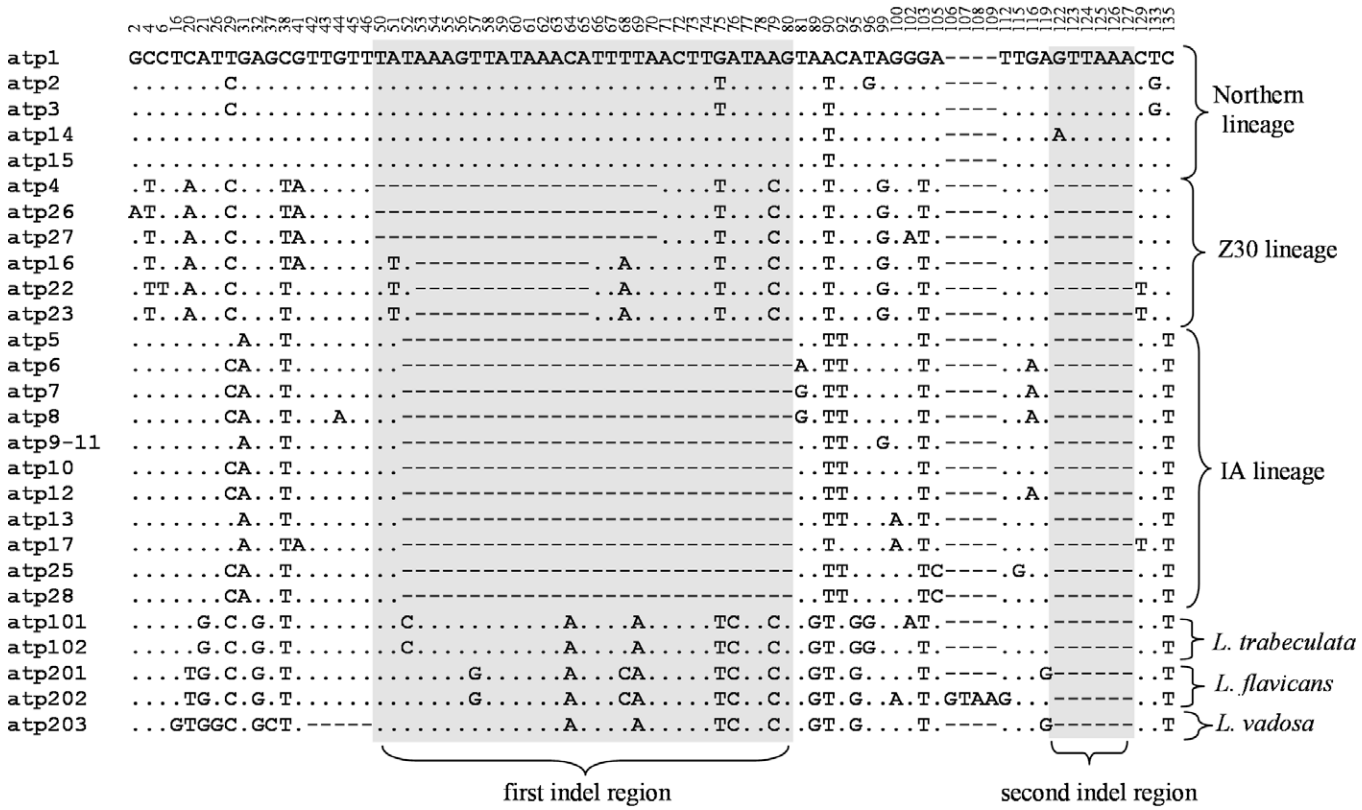

Fig. 1. Alignment of the 22 atp8/trnS haplotypes obtained for *L. nigrescens* and the outgroup species (multilocus approach data set). Only polymorphic sites are shown. The sequences are grouped by similarity for indel polymorphism, and lineages within *L. nigrescens* are indicated based on the phylogenetic tree (see Fig. 2). The two indel regions showing polymorphism within *L. nigrescens* are indicated by shaded area.

was similar or higher than the divergence between recognized sister species. For ITS1, the divergence was of the same order of magnitude between the IA and PP lineages (2.7%) as between *L. trabeculata* and any *L. nigrescens* lineage (2.5–3%) or even between *L. vadosa* and *L. corrugata*, two species separated by the South Pacific (2.7%, Fig. 2). For atp8/trnS, the divergence (calculated excluding indel sites) among clades within *L. nigrescens* was nearly twice as high as the divergence between *L. flavicans* and *L. trabeculata* (6.3–7.5% vs. 3.8%, respectively; Fig. 2) or the divergence between *L. flavicans* and *L. vadosa* (4.0%, Fig. 2). All phylogenetic reconstructions showed consistently larger branches for *L. nigrescens* alleles than for other species of *Lessonia* (Figs. 2 and 3). Within *L. nigrescens*, the IA alleles were consistently closer to the outgroup species than the PP alleles (Figs. 2 and 3).

Divergence time between PP and IA was estimated using the indirect calibration of the molecular clock calculated for the RuBisCo spacer (ranging from 0.53% to 0.80% Myr^{-1}). As sequence divergence varied from 0.2% to 0.9% between PP and IA haplotypes, the divergence time between the two lineages was estimated to range between 0.250 and 1.698 Myr.

3.4. Lineages with geographically restricted distributions and absence of admixture

The multilocus approach allowed detecting the presence of three clades for the mitochondrial marker, each clade showing a distinct distribution range (Supplementary material-Fig. S1). However, by increasing the sample size to about 30 individuals per location, we defined more precisely the distribution of each clade. Nine of the recovered haplotypes were absent of the multilocus approach data set, but the phylogenetic relationships described previously did not change. Each of these new haplotypes (atp29–atp35, atp28 and atp39) differed from haplotypes detected in the multilocus data set by only one or two base pairs (Fig. 4; GenBank Accession Nos. FJ410117–FJ410125).

The distribution ranges of the Northern and the Z30 clades did not overlap, and displayed a narrow and abrupt genetic discontinuity zone located between 27°12′S and 27°41′S (Fig. 4 and Supplementary material-Fig. S1). In contrast, the ranges of Z30 and IA clades overlapped in a region located between 29°03′S and 30°14′S. This overlapping region was characterized by the occurrence of several patches composed exclusively of IA haplotypes (COZ at 29°57′S, IPA at 29°35′S and ACE at 29°03′S, Fig. 4) scattered within the geographic area of the Z30 clade. It is important to notice that, in both transition zones, all populations were made of haplotypes from just one clade (Fig. 4). This absence of admixture among clades was retrieved for each of the three other markers used in the multilocus approach (Supplementary material-Fig. S1).

3.5. Polymorphism within Lessonia nigrescens clades and populations

Globally, the SSCP method was able to clearly discriminate between different sequences, i.e. atp8/trnS mitochondrial haplotypes, within and among populations. Indeed, most SSCP profiles (15 over 18) corresponded to a single sequence. Two of the three remaining profiles corresponding to more than one haplotype could be subsequently identified as atp5 from atp10 and atp12 from atp13 using RFLP screening. Only one profile (profile C) was difficult to identify. This profile, exclusively found in the Z30 region, corresponded to three distinct haplotypes, differing by one base pair (haplotypes atp4, atp27 and atp29). However, as the atp4 haplotype was the most frequent (observed in 13 out of 19 sequences analyzed for

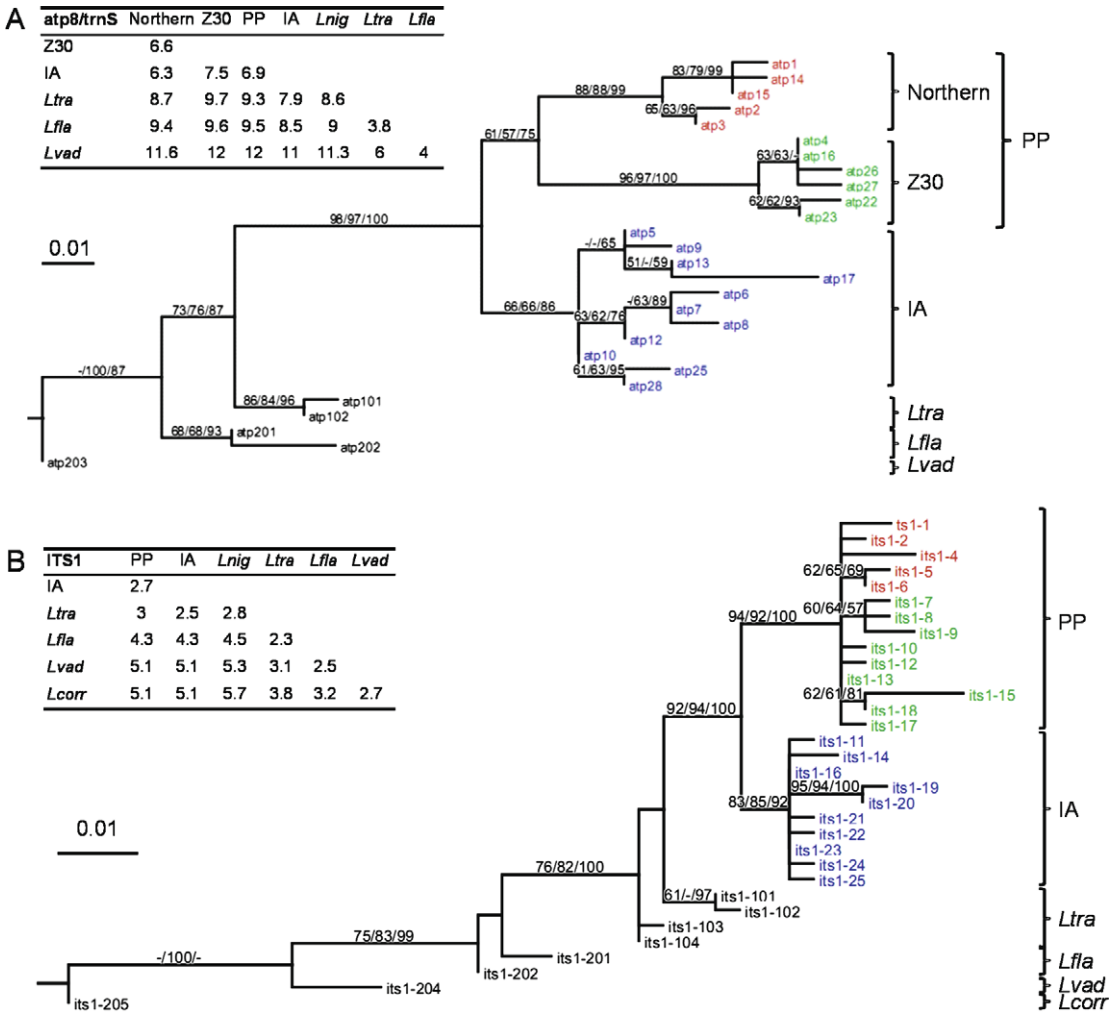

Fig. 2. Maximum likelihood trees based on atp8/trnS and ITS1 for *L. nigrescens* and corresponding *p*-distances. (A) atp8/trnS, data set of the multilocus approach, indels considered as missing data, (B) ITS1 data set. Support values are presented as maximum parsimony bootstraps, maximum likelihood bootstraps and Bayesian posterior probabilities, respectively, and "–" indicates <50% support in a particular analysis. The color of allele names represents the atp8/trnS clade of the individuals showing these alleles (see Supplementary Material-Fig. S1) and the outgroup species are indicated. The matrices show the *p*-distances calculated among clades excluding indels, for both atp8/trnS and ITS1 markers.

this profile), and occupied a central position on the network reconstruction (Fig. 4), we considered all individuals having this particular profile as having the atp4 haplotype for the calculation of the diversity indices. This approach certainly underestimated the polymorphism within this region.

A total of 31 haplotypes were recovered from the 1051 analyzed individuals. Northern and IA clades were sampled along a comparable coastline distance (1416 and 1815 km, respectively). The IA clade presented a larger number of haplotypes and higher nucleotide (π) and gene (H) diversity than the Northern clade (Table 3). However, since sampling effort was not equivalent in both regions, we used a re-sampling method to estimate the diversity indices within the IA clade (100 random re-sampling of seven out of 17 locations). Re-sampling showed that Northern and IA clades were similar in terms of gene diversity (the higher gene diversity of IA clade can only be explained by the higher sampling effort; data not shown). The nucleotide diversity remained slightly higher for IA clade than for Northern clade but both values showed a high standard variation (Table 3, data not shown for re-sampling). This reflected the high structure in both clades with the presence of rare haplotypes only in the IA clade (Fig. 4). Lowest gene diversity was observed for the Z30 clade. This, however, may be the consequence of an underestimation of polymorphism, as rare haplotypes (atp27 and atp29) were not detected by SSCP. When considering the contiguous stretch of eight indels observed within Z30 clade haplotypes as a unique mutation event, the nucleotide diversity was lower than for the two other clades (Table 3).

For the AMOVA analyses, different hierarchical models were tested: populations were grouped accordingly to their geographic locations (i.e. localizing the transition zone at 30°S or at 33°S) or to their phylogenetic affinities (i.e. the three phylogenetic clades observed for atp8/trnS). Since phylogenetic clades presented a higher significance and explained a most important part of the variance, we chose to use this last model of grouping. Most of the mitochondrial genetic variation in *L. nigrescens* was explained by the differentiation between clades (88.9%, Table 4; 90.2% when indels were excluded, data not shown). However, differentiation among locations within a clade was also highly significant and accounted for more than 10% of the observed genetic variation at atp8/trnS (Table 4). Taking into account the substitution model obtained with ModelTest did not change the results (data not shown).

In contrast to the relatively high polymorphism values observed at the clade level, the polymorphism within locations was surprisingly low. The number of locations showing more than one mitochondrial haplotype was very limited (11 out of 34 locations, Table 3). In addition, most of the polymorphic locations exhibited

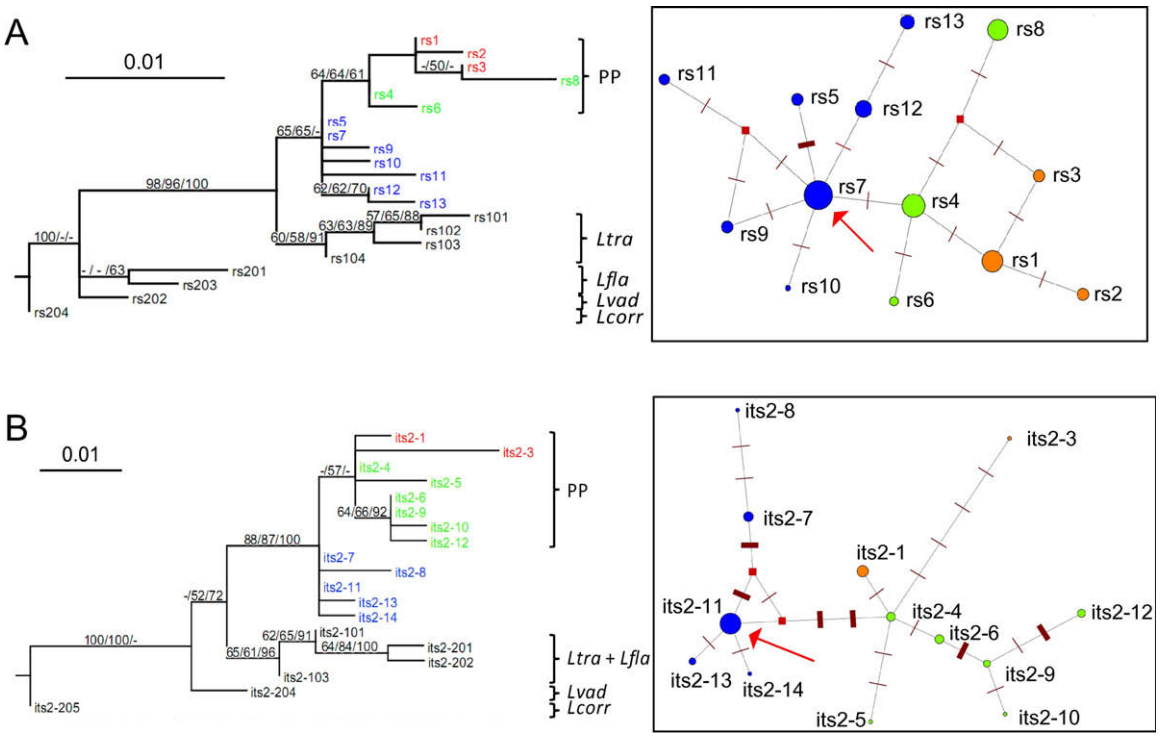

Fig. 3. Maximum likelihood trees and unrooted networks for RuBisCo spacer haplotypes (A) and ITS2 ribotypes (B) within *L. nigrescens*. For tree legend, see Fig. 2. In networks, red squares represent hypothetical haplotypes or ribotypes not detected in this study and red bars indicate mutations (narrow bars: substitutions, large bars: deletion). The size of the circle is proportional to the number of individuals bearing a given allele. The colors of pie-charts correspond to the atp8/trnS clade of the individuals (see Fig. 2). Arrows indicate the ancestral alleles for each network (ancestrally determined with rooted networks, not shown).

a predominant haplotype, with generally one, and up to three, rare haplotypes differing by one base pair from the common haplotype (Fig. 4). This was reflected by the low within-location gene and nucleotide diversity values combined with high standard deviations (Table 3). However, three locations showed a distinct pattern exhibiting two haplotypes with similar frequencies: SLD in the Northern clade, and MEH and PUC from the southern part of the IA region (Table 3 and Fig. 4). In addition to the low polymorphism within populations, *L. nigrescens* was characterized by an important proportion of private haplotypes, i.e. found in only one location (4 out of 6 haplotypes in the Northern clade, 3 out of 7 haplotypes in Z30 clade and 11 out of 18 haplotypes in IA clade). Distances among locations sharing haplotypes were generally low, being less than 150 km of coastline in most cases. The four exceptions concerned haplotypes from the southern part of the IA clade distribution: atp6, atp7 and atp8 were shared among locations separated by 270–347 km (PICHI–GBN, Fig. 4). Within the Z30 clade, the atp4 haplotype was shared between populations separated by 132 km, and this was verified by the sequencing approach. It was the only case of haplotype shared among non-adjacent locations (the TON/GUANA/OTO group of locations is separated from the TBL/CHS/CHN group by TEA, ARY and COZ, Fig. 4). Within each clade, Mantel tests were significant (*P*-value of 0.009, 0.004 and 0.014 for Northern, Z30 and IA clades, respectively, Fig. 5). An isolation by distance pattern explained a larger part of the variance in the Northern clade ($R^2 = 0.55$) than in the IA clade ($R^2 = 0.15$, Fig. 5). LM was highly differentiated from all other locations, greater than expected by the isolation-by-distance pattern among the other locations of the IA clades. Removing this location increased the R^2 to 0.44 (*P*-value <0.001).

Mismatch distributions were clearly unimodal for the IA haplotypes, whereas the Northern clade showed a bimodal mismatch distribution (Fig. 6). Both sudden demographic expansion and spatial expansion models fitted to the observed IA mismatch with reasonably high bootstrap support (0.795 and 0.781, respectively), with $\tau = 1.4$ and 1.3, respectively. For the Northern clade, the sudden demographic expansion had negligible bootstrap support (0.37), but higher support (0.63) was found for the spatial expansion model, with $\tau = 3.0$.

4. Discussion

Our study demonstrates the presence of two main divergent lineages within the kelp *Lessonia nigrescens*, one on each side of the debated biogeographic 30°S transition zone. Based on a sampling scheme that covered most of the distribution range of the species, the genetic markers from the three genomic compartments revealed that this southern Pacific transition zone corresponds to a phylogenetic break. However, in spite of their congruent response on the phylogeographic structure, important differences between markers became apparent in relation to the intensity of the genetic divergence. Furthermore, we found discrepancies among markers regarding the putative presence of a second genetic discontinuity at 27°S. The possible scenarios responsible for the origin of these phylogeographic patterns and the mechanisms that might be involved in maintaining the geographic distribution of lineages, and of alleles within lineages, are discussed below.

4.1. Genetic discontinuity at 30°S

All markers consistently showed the presence of a genetic break within *L. nigrescens* differentiating the Peruvian Province (PP) from the Intermediate Area (IA) despite some difference in the topologies. This consistency among markers strongly supports the involvement of an external factor as the main cause of divergence among lineages. Selective or drift effects on a particular part of the genome can thus be discarded as putative mechanisms (see Ballard and Rand, 2005; Irwin, 2002; Kuo and Avise, 2005) responsible for

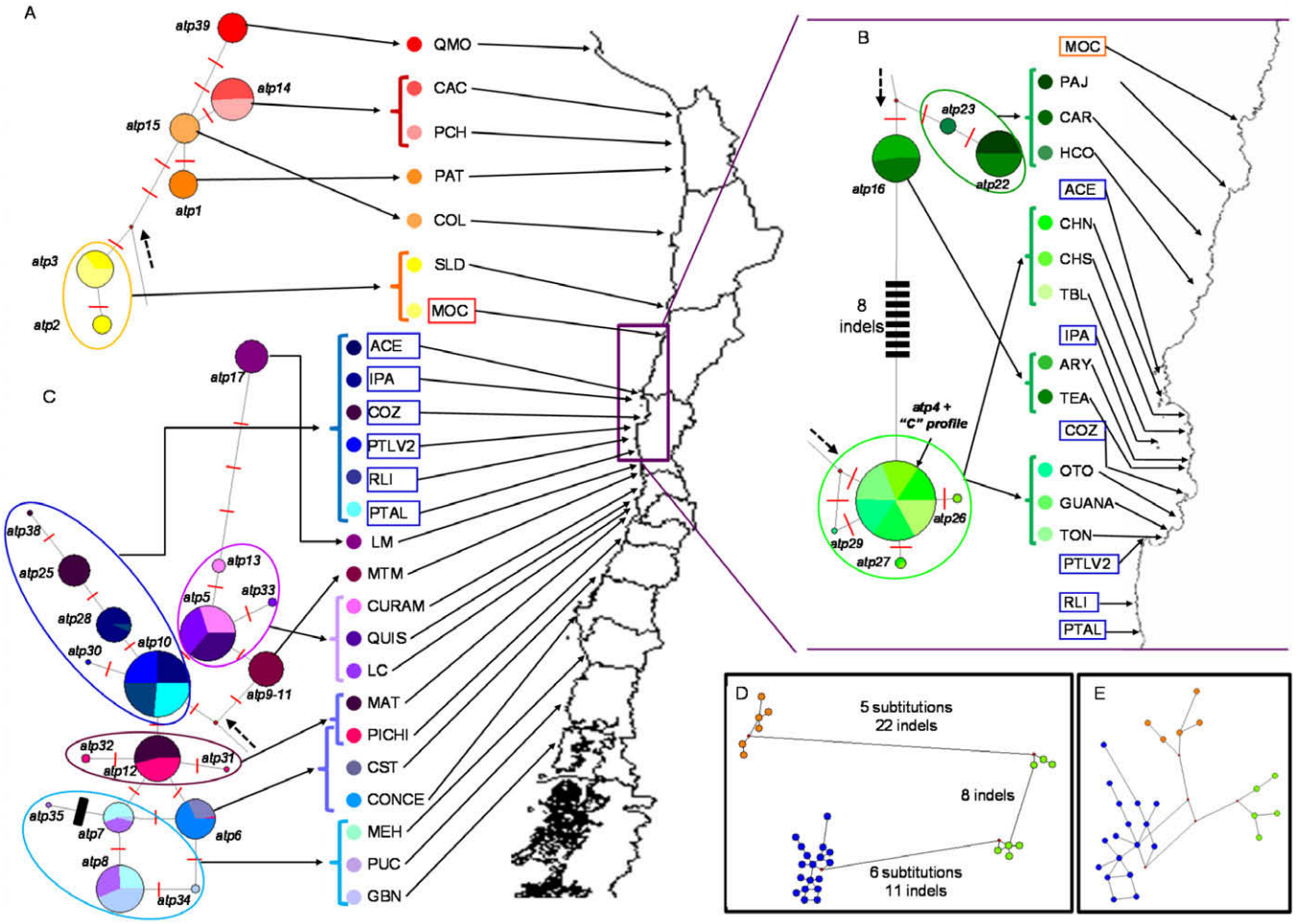

Fig. 4. Haplotype networks of atp8/trnS marker within each clade, for the population-level study. (A) Northern clade, (B) Z30 clade and (C) IA clade. Relations among clades are shown in unrooted networks including (D) and excluding (E) indel sites. Location of the haplotypes on the map is indicated by arrows and with the location names (see Table 1 for abbreviations). See also legend of Fig. 3 for network components. Individuals showing a profile "C" on SSCP gels are represented as individuals having the atp4 haplotype (bold letters).

Table 3
Genetic diversity within *L. nigrescens*. %π, percentage of nucleotide diversity; *H*, mean (and standard deviation) gene diversity calculated overall individuals belonging to each clade, over location within clade and within each location (excluding those with less than 28 individuals, i.e. HCO and CST). Only polymorphic locations are shown. Within Z30 clade, the eight contiguous indels are considered as a unique mutation event.

atp8/trnS clade and *polymorphic location*	No individuals (No locations)	No haplotypes	%π (SD)	*H* (SD)
Northern clade	206 (7)	6	1.6116 ± 0.9658	0.8072 ± 0.0101
SLD	29	2	0.3305 ± 0.3198	0.5123 ± 0.0311
Mean over Northern locations	29.4	1.14	0.0472 ± 0.1249	0.0732 ± 0.1936
Z30 clade	308 (10)	6	1.1151 ± 0.7537	0.5690 ± 0.0224
CHS	30	2	0.1006 ± 0.1744	0.1287 ± 0.0792
Mean over Z30 locations	30.8	1.30	0.0101 ± 0.0318	0.0129 ± 0.0407
IA clade	511 (17)	18	2.0360 ± 1.2217	0.8762 ± 0.0060
COZ	28	2	0.0595 ± 0.1364	0.0714 ± 0.0652
PTLV2	30	2	0.0556 ± 0.1313	0.0667 ± 0.0613
RLI	29	2	0.1108 ± 0.1895	0.1330 ± 0.0814
CURAM	30	2	0.2395 ± 0.2912	0.2874 ± 0.0917
QUIS	30	2	0.1073 ± 0.1860	0.1287 ± 0.0792
PICHI	30	4	0.2184 ± 0.2761	0.2506 ± 0.1017
MEH	30	2	0.4291 ± 0.4139	0.5149 ± 0.2680
PUC	30	3	0.4559 ± 0.4300	0.5034 ± 0.0642
GBN	30	3	0.1628 ± 0.2338	0.1908 ± 0.0928
Mean over IA locations	30.1	1.72	0.1397 ± 0.1892	0.1263 ± 0.1694

the detected genetic discontinuity between the two south-eastern Pacific biogeographic regions.

The genetic discontinuity was supported by high bootstrap values and posterior probabilities and long branches for all markers, and a reciprocal monophyly for the faster evolving markers (atp8/trnS and ITS1). However, the slower evolving markers (ITS2 and RuBisCo spacer) showed a slightly different topology, with a monophyletic PP lineage embedded in the IA lineage. The comple-

Table 4
Analysis of molecular variance (AMOVA) for atp8/trnS population analysis excluding locations with less than 28 individuals (i.e. HCO and CST).

Source of variation	Degree of freedom	Sum of squares	Variance components	Percentage of variation (%)	*P*-value
Among Northern, Z30 and IA clades	2	8860.756	13.76594	88.86	<0.00001
Among populations within clades	31	1624.550	1.68507	10.88	<0.00001
Within populations	961	40.899	0.04127	0.27	<0.00001
Total	1024	10477.782	15.49227		

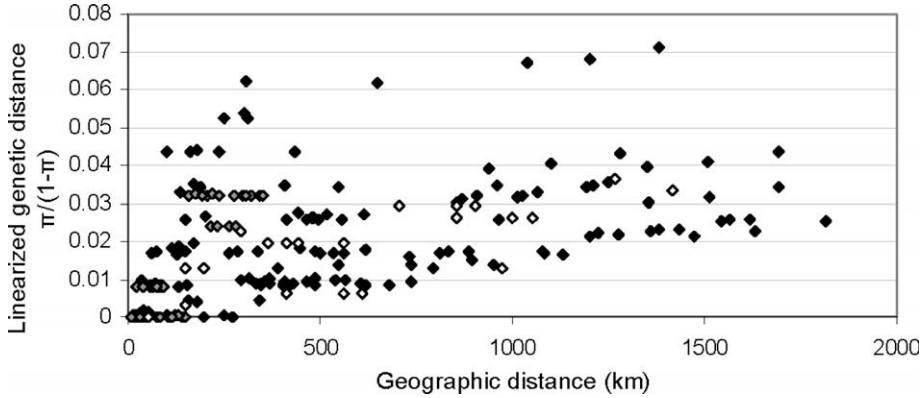

Fig. 5. Genetic differentiations of *L. nigrescens* locations within the three mitochondrial clades (black, grey and white symbols are for IA, Z30 and Northern clades, respectively). Pairwise genetic distances, represented as $\pi/(1-\pi)$ are plotted against geographic distances.

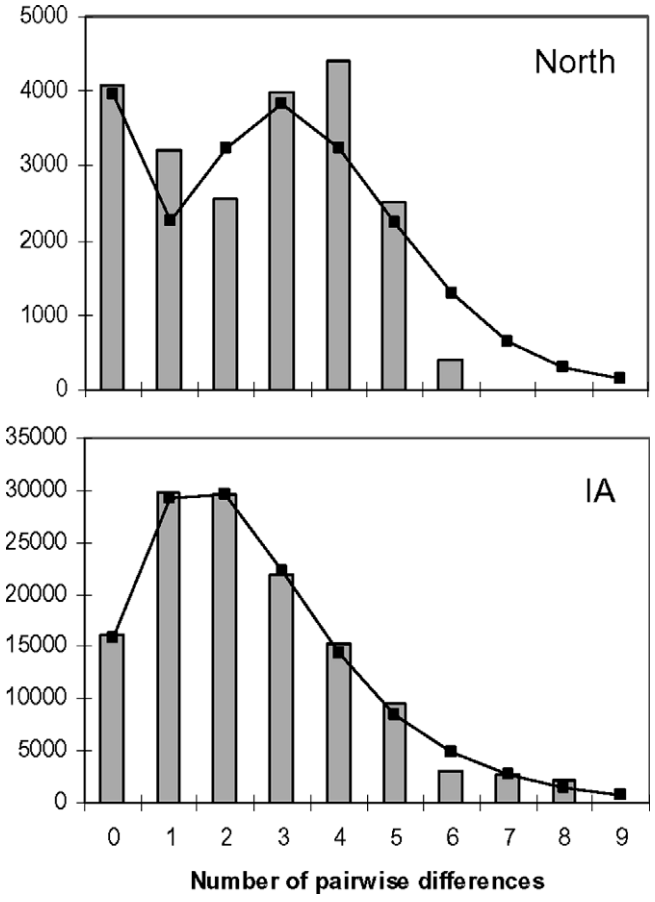

Fig. 6. Mismatch distributions of the Northern and IA mitochondrial clades of *L. nigrescens*. The observed distributions (bars) are contrasted to their expected distribution under a model of spatial expansion (solid lines).

mentary information given by the network of haplotypes/ribotypes indicates that the absence of reciprocal monophyly is almost certainly linked to the retention of ancestral alleles in the IA lineage. The monophyletic PP lineage nested within the other group of alleles may thus be an intermediate stage prior to a complete reciprocal monophyly (Omland et al., 2006). This kind of pattern can emerge by genetic drift that progressively eliminates ancestral alleles in some populations faster than in others due to either smaller population size or to demographic fluctuations. In this study, we interpreted the difference in tree topology as the consequence of differential mutation rates. Indeed, data from the literature suggest that ITS1 has a higher mutation rate than ITS2 (e.g. for the kelp *Macrocystis* sp.; Coyer et al., 2001). Furthermore, RuBisCo spacer is generally described as more conserved than ITSs, as demonstrated for the kelp *Undaria* (Yoon and Boo, 1999) and in other species of Phaeophyceae (Harvey and Goff, 2006). In addition, comparison of sequence variation among nine Laminarian and three Fucoid species confirmed that RuBisCo spacer was also more conserved than atp8/trnS (Engel et al., 2008).

4.2. Timing of the divergence among L. nigrescens lineages and possible scenarios

For the two reciprocally monophyletic markers, the distances among lineages were of the same order than the distances among other *Lessonia* species included in this study. For instance, the ITS1 sequence divergence was as high between IA and PP lineages as between species from both sides of the Pacific Ocean, *L. vadosa* and *L. corrugata*. More generally, ITS1 divergence among PP and IA lineages was of similar importance as what has been described between closely related kelp species, such as between the European *Laminaria digitata* and *Laminaria hyperborea* (3.1% of divergence for ITS1 and ITS2; Erting et al., 2004), or between the Japanese *Laminaria* (3.4–4.2% for ITS1; Yotsukura et al., 1999). Moreover, we neither observed introgression between PP and IA lineages nor mixture of lineages within a single location, regardless the number of individuals. Even in the common case of multiple copies of the ITS region observed after cloning (Coyer et al., 2001; Lane et al., 2007), the different sequences recovered within-individuals were always from the same lineage. This absence of gene flow among

lineages strongly supports the occurrence of two cryptic species that diverged long time ago.

Unfortunately, our capacity to estimate the time since these two lineages within *L. nigrescens* separated is limited due to the absence of fossil records or other recorded geological or paleontological events. The indirect estimation of a molecular clock for the RuBisCo spacer marker suggests that the divergence arose 0.250–1.698 Myr BP. Despite the low precision of the estimated timing, we can conclude that the divergence among lineages within *L. nigrescens* is ancient, close to the divergence from the sister species *L. trabeculata*, and that it originated long before the Last Glacial Maximum, which is the most common historical factor investigated in marine phylogeography (Avise, 2000; Dawson, 2005; Maggs et al., 2008).

What is the scenario for such a genetic divergence? The monophyletic PP lineage embedded within IA lineage for two out of four markers strongly supports a scenario of sudden range expansion from a reduced, marginally distributed group of alleles of the IA lineage. In this case, strong genetic drift could have occurred not only because of the founder effect, but also during the range expansion by gene surfing (Excoffier and Ray, 2008), resulting in strong genetic differentiation between the source southern population and the newly colonized areas. Mismatch analyses at the population-level for atp8/trnS further support a past spatial expansion in the Northern clade, likely linked to the northward colonization. Such a pattern is expected under a budding or a parapatric speciation process, rather than a persistent vicariance (Funk and Omland, 2003). Budding speciation (or peripatric speciation) is a particular case of vicariance in which populations along the periphery of a species range become spatially isolated (Funk and Omland, 2003). On the other hand, parapatric speciation involves the evolution of adaptations in marginal environments and/or changes in ecological conditions that allow the colonization of new areas. Both speciation processes involve a range expansion from a subset of marginal populations, which fits well with the observed data. Long-term vicariance is hardly supported not only by this phylogenetic pattern but also because, contrary to most coastal biogeographic transitions studied around the world where barriers to dispersal have been reported as the main cause of genetic discontinuities, such evidences are lacking in the oceanographic, geological or paleontological record around the 30–33°S southeastern Pacific (Camus, 2001).

Two scenarios can explain how colonization of the northern region may have originated the current genetic discontinuity: (1) a change in environmental conditions, and (2) an adaptation to the environmental conditions of the northern region. Paleo-oceanographic data are needed to determine the date, frequency and magnitude of environmental changes that might have occurred along the Chilean coast between 0.250 and 1.698 Myr ago. Currently, the 30°S region is exposed to one of the two maximum wind stress for upwelling conditions present along the Chilean coast (Thiel et al., 2007), which has been used as a potential explanation for important changes in recruitment patterns of several invertebrate species between 30 and 32°S (Broitman et al., 2001; Navarrete et al., 2005). The 30°S region (29–32°S) separates a wide northern zone (800–1000 km) with weak but persistent winds that favor upwelling, from a southern zone where winds, though stronger, are more variable (Hormazabal et al., 2004). There is also evidence of a global persistence in the currents pattern since the establishment of the Humboldt Current System (HCS), in particular regarding the presence of upwelling regimes that bring cold and nutrient-rich waters to coastal areas (Thiel et al., 2007) and favor the presence of kelp populations. The emergence of the HCS is therefore a potential factor allowing the range expansion of cold-temperate species towards the North. There are, however, strong discrepancies among authors regarding the establishment of this complex oceanographic system, situating it between 1.6 and 35 Myr BP (reviewed in Camus, 2001). This provides only a marginal overlap with the estimated timing for the origin of the genetic divergence in *L. nigrescens*.

The only other species studied for its phylogeography in this region, the benthic gastropod *Concholepas concholepas*, showed no genetic discontinuity along its entire range of distribution (Cárdenas et al., 2009). However, in this invertebrate characterized by long-distance larval dispersal, the authors suggested that a demographic expansion from only one haplotype likely erased the signature of any pre-existent genetic structure. The onset of the demographic expansion of *C. concholepas* has been estimated at around 400,000 years BP based on mtDNA COI mismatch distribution (Cárdenas et al., 2009). This expansion was likely contemporary to the favorable climatic conditions during the period of the marine isotope stage MIS 11 (Ortlieb et al., 2003), the longer and warmer interglacial period that occurred in the Pleistocene. It is thus probable that the emergence of divergent lineages in *L. nigrescens* occurred earlier than 400,000 years BP.

On the other hand, an adaptation to particular environmental conditions north of 30°S is a scenario that requires the assumption of strong selective factor(s) that would have affected the entire genome. Selection is generally considered too weak in marginal populations to lead to adaptation because of strong effects of genetic drift and immigration load from central populations (Bridle and Vines, 2007). A selective sweep associated with a particularly beneficial mutation in a northern population is a hypothesis that cannot be ruled out as this phenomenon is, indeed, expected to affect the entire genome due to strong founder effects. Certainly such a situation would not be exclusive of the colonization scenario, in particular if the selective sweep occurred in a marginal population at the northern limit of IA lineage. Regardless the specific circumstances that led to range expansion towards the north, this scenario is an interesting case of probable budding speciation, leading to a genealogically nested PP lineage within IA lineage for low-evolving markers. Such evolutionary processes may be common (see for review Funk and Omland, 2003) and is expected to result from a combination of drift and selection in marginal populations at the species range limits. The examples generally concern speciation after colonization of islands distant from the continent (e.g. in Macaronesia for a plant species: Vanderpoorten and Long, 2006) or from other islands (e.g. for a Lepidoptera species in Galapagos Islands: Schmitz et al., 2006), or the case of a generalist species budding off a specialist phytophagous insect species (Morse and Farrell, 2005). To our knowledge, this process has not yet been described in the marine organisms.

4.3. Discordant patterns: a second genetic discontinuity at 27°S?

In addition to the major phylogenetic break present in all markers, atp8/trnS showed a second phylogenetic discontinuity around 27°S, as seen by a split of the PP lineage into a Z30 clade and a Northern clade, both statistically well-supported. These two subclades diverge in terms of both indel polymorphism and substitution polymorphism. Moreover, the divergence between these two sub-clades was of the same order as the divergence between IA and each PP sub-clade, suggesting also an ancient origin of this discontinuity. However the disjoint distribution of these two subclades, with an abrupt discontinuity between 27°12′S and 27°41′S, does not correspond either to a known biogeographic or ecological transition zone (Camus, 2001; Thiel et al., 2007).

The discrepancy between the mitochondrial marker and markers from other cell compartments raises the question whether this second genetic discontinuity is the consequence of evolutionary forces that affected only the mitochondrial genome. There are indeed increasing evidence on how selection can shape the evolution

of the mitochondrial genome (Ballard and Rand, 2005; Bazin et al., 2006). In particular, because mitochondria are involved in important physiological functions, such as cellular respiration, selective forces may affect the atp8/trnS intergenic spacer by hitchhiking. In this context, the 27°S discontinuity could reflect some kind of adaptation to an environment more influenced by El Niño Southern Oscillations (ENSO), or to higher sea surface temperature (Castilla and Camus, 1992; Thiel et al., 2007). Studies on kelp physiology in different environments and on the role of the mitochondrial genome in potential adaptations to specific environments are needed at this point. An alternative hypothesis is that this phylogeographic discontinuity at 27°S is of stochastic origin, i.e. determined by genetic drift in a species of very low dispersal capacity. It has been shown that the mitochondrial markers, because of their smaller effective size, are more susceptible to show 'haphazard" phylogeographic discontinuity than nuclear markers, particularly for low dispersal species (Irwin, 2002; Kuo and Avise, 2005). The absence of alleles shared between the Z30 and Northern sub-clades for atp8/trnS but also for the other three markers, and the high number of individuals analyzed in this region, suggest an absence of gene flow across the 27°S.

4.4. Limited gene flow within lineages and a particular structure in the transition zone

Within each mitochondrial clade, the population-study analyses confirmed a previous report (Faugeron et al., 2005) that dispersal is very limited in this species complex. In the transition zone dominated by individuals belonging to the PP lineage, several patches (populations) were found to be exclusively made of individuals of the IA lineage. We hypothesize that rare long-distance dispersal events from the IA zone are at the origin of the colonization of these new locations. This is consistent with the general northward trend of coastal currents and the presence close to the shore of the Humboldt Current (also of northward direction) in this area (Thiel et al., 2007). It is difficult however to discriminate the effect of this scenario from range shifts that likely occurred during the history of the species. What remains surprising is that, probably limited by the reduced dispersal capacity of the species, both lineages did not expand their range beyond the narrow overlapping area (29°03′–30°14′S).

Such a low gene flow is an important force that may have contributed to the maintenance of the genetic signature for a long period of time (Irwin, 2002). It might also have contributed to the reinforcement of the genetic divergence by limiting the possibility of hybridization and introgression. Indeed, no mixed multilocus genotypes (i.e. those containing alleles from both PP and IA) have been observed despite the intensive sampling of the transition area. In addition, and consistent with the general pattern of monomorphism within populations, each sampled location of the transition area was either fixed for the PP or the IA alleles. Thus, this transition area does not correspond to a hybrid zone, but rather to a contact zone with an overlapping area between two completely isolated species. Whether this isolation is due to restricted gene flow and/or to reproductive isolation remains to be tested. Our study however strongly ascertains that the two lineages correspond operationally to two fully isolated species.

4.5. Conclusions and perspectives on the maintenance of the 30°S biogeographic transition

The PP and IA lineages of *L. nigrescens* show a disjoint distribution, with a narrow patchy overlapping area between 29°03′S and 30°14′S, and this genetic discontinuity matches exactly the location of the biogeographic transition proposed for the marine flora and fauna. The presence of the 30°S biogeographic transition appears to be the result of both historical and contemporary processes. Among the possible historical scenarios for such a genetic discontinuity, large-scale vicariance is poorly supported because of a lack of known barrier to dispersal and the tree topology obtained for two of the four markers. Rather, genetic data support a northward range expansion. The deep genetic divergence and the lack of evidence for introgression or hybridization demonstrate the occurrence of two cryptic *L. nigrescens* species that likely evolved through parapatric or budding speciation. The occurrence of such evolutionary processes in the biogeographic transition strongly suggests that major ecological shifts may have taken place in this region, and likely limited the range distribution of many species. The exact geographic match between the 30°S biogeographic transition and the genetic discontinuity observed in *L. nigrescens* sheds light to our understanding of the biogeography of the south-eastern Pacific. Some ecological or oceanographic contemporary constraints to dispersal and colonization across the 30°S seem to remain affecting many species, as indicated by breaks in recruitment patterns in several invertebrate species (Broitman et al., 2001; Navarrete et al., 2005). While located at easily-reached dispersal distances in the contact zone, the two cryptic species of *L. nigrescens* were never observed together within the same site. The absence of mixed populations raises stimulating lines of research on the maintenance of each exclusive pattern between the two genetic entities.

Finally, management policies of this economically important resource should take into account that *L. nigrescens* complex is formed by two isolated genetic stocks. In particular, most of the harvesting pressure and most of the environmental stresses from human pollutions or from ENSO are occurring in the northern part of the country (Vásquez, 2008), more specifically north of the 30°S. These perturbations are thus mainly affecting the northern species. Restoration efforts currently ongoing and stock management should care about the genetic status of the target resource.

Acknowledgments

We are particularly grateful to all who helped with collecting samples: J. Beltran, C. Camus, A. Gamarra, M.-L. Guillemin, E. Martínez, S. Navarrete, C. Olivares, V. Oppliger, A. Peters, J. Plana, J. Vásquez and A. Vega. We also thank C. Daguin, G. Peralta and J. Tapia for their assistance in the lab, C.R. Engel and M. Voisin for the development of SSCP method on the study species and S. Plouviez for her assistance with ITS cloning. We particularly appreciated insightful and constructive comments from C. Destombe, S. Krueger and two anonymous reviewers. This research was supported by a doctoral grant from the French Ministry of Education and Research (MENRT) to F. Tellier, FONDECYT Grant 1060493 to S. Faugeron and ANR-ECOKELP (ANR 06 BDIV 012) to M. Valero. A. Meynard received a pre-doctoral grant from the Master Program Region Metropolitana (Chile)-Region Ile de France (France). Additional support from the programs "Collège Doctoral Franco-Chilien" and "ARCUS" of the French Ministry of Foreign Affairs, by the ECOS-CONICYT C03B04, FONDAP-FONDECYT 1501-0001 and by the Laboratoire International Associé "Dispersal and Adaptation of Marine Species" (LIA DIAMS) is also acknowledged.

Appendix A. Supplementary data

Supplementary data associated with this article can be found, in the online version, at doi:10.1016/j.ympev.2009.07.030.

References

Avise, J.C., 2000. Phylogeography: The History and Formation of Species. Haward University Press, Cambridge.

Ballard, J.W.O., Rand, D.M., 2005. The population biology of mitochondrial DNA and its phylogenetic implications. Ann. Rev. Ecol. Syst. 36, 621–642.
Ballard, J.W.O., Whitlock, M.C., 2004. The incomplete natural history of mitochondria. Mol. Ecol. 13, 729–744.
Bandelt, H.J., Forster, P., Röhl, A., 1999. Median-joining networks for inferring intraspecific phylogenies. Mol. Biol. Evol. 16, 37–48.
Bazin, E., Glémin, S., Galtier, N., 2006. Population size does not influence mitochondrial genetic diversity in animals. Science 312, 570–572.
Bolnick, D.L., Fitzpatrick, B.M., 2007. Sympatric speciation: models and empirical evidences. Ann. Rev. Ecol. Syst. 38, 459–487.
Bridle, J.R., Vines, T.H., 2007. Limits to evolution at range margins: when and why does adaptation fail? Trends Ecol. Evol. 22, 140–147.
Broitman, B.R., Navarrete, S.A., Smith, F., Gaines, S.D., 2001. Geographic variation of southeastern Pacific intertidal communities. Mar. Ecol. Prog. Ser. 224, 21–34.
Castilla, J.C., Camus, P.A., 1992. The Humboldt-El Niño scenario: coastal benthic resources and anthropogenic influences, with particular reference to the 1982/83 ENSO. *S. Afr. J. Mar. Sci.* 12, 703–712.
Camus, P.A., 2001. Biogeografía marina de Chile continental. Rev. Chil. Hist. Nat. 74, 587–617.
Cárdenas, L., Castilla, J.C., Viard, F., 2009. A phylogeographic analysis across three biogeographic provinces of the south-eastern Pacific: the case of the marine gastropod *Concholepas concholepas*. J. Biogeogr. 36, 969–981.
Chapman, A.R.O., 1993. 'Hard' data for matrix modelling of *Laminaria digitata* (Laminariales, Phaeophyta) populations. Hydrobiologia 260 (261), 263–267.
Connolly, S.R., Menge, B.A., Roughgarden, J., 2001. A latitudinal gradient in recruitment of intertidal invertebrates in the northeast Pacific Ocean. Ecology 82, 1789–1813.
Corpet, F., 1988. Multiple sequence alignment with hierarchical clustering. Nucleic Acids Res. 16, 10881–10890.
Coyer, J.A., Smith, S.J., Andersen, R.A., 2001. Evolution of *Macrocystis* spp. (Phaeophyceae) as determined by ITS1 and ITS2 sequences. J. Phycol. 37, 574–585.
Dawson, M.N., 2001. Phylogeography in coastal marine animals: a solution from California? J. Biogeogr. 28, 723–736.
Dawson, M.N., 2005. Incipient speciation of *Catostylus mosaicus* (Scyphozoa, Rhizostomeae, Catostylidae), comparative phylogeography and biogeography in south-east Australia. J. Biogeogr. 32, 515–533.
Destombe, C., Douglas, S.E., 1991. Rubisco spacer sequence divergence in the rhodophyte alga *Gracilaria verrucosa* and closely related species. Curr. Genet. 19, 395–398.
Engel, C.R., Billard, E., Voisin, M., Viard, F., 2008. Conservation and polymorphism of mitochondrial intergenic sequences in brown algae (Phaeophyceae). Eur. J. Phycol. 43, 195–205.
Erting, L., Daugbjerg, N., Pedersen, P.M., 2004. Nucleotide diversity within and between four species of *Laminaria* (Phaeophyceae) analysed using partial LSU and ITS rDNA sequences and AFLP. Eur. J. Phycol. 39, 243–256.
Excoffier, L., 2004. Patterns of DNA sequence diversity and genetic structure after a range expansion: lessons from the infinite-island model. Mol. Ecol. 13, 853–864.
Excoffier, L., Laval, G., Schneider, S., 2005. Arlequin ver. 3.0: an integrated software package for population genetics data analysis. Evol. Bioinform. Online 1, 47–50.
Excoffier, L., Ray, N., 2008. Surfing during population expansions promotes genetic revolutions and structuration. Trends Ecol. Evol. 23, 347–351.
Faugeron, S., Martínez, E.A., Correa, J.A., Billot, C., 2005. Long-term copper mine waste disposal in northern Chile associated with gene flow disruption of the intertidal *Lessonia nigrescens*. Mar. Ecol. Prog. Ser. 288, 129–140.
Felsenstein, J., 1985. Confidence limits on phylogenies: an approach using the bootstrap. Evolution 39, 783–791.
Fitzpatrick, B.M., Fordyce, J.A., Gavrilets, S., 2008. What, if anything, is sympatric speciation? J. Evol. Biol. 21, 1452–1459.
Funk, D.J., Omland, K.E., 2003. Species-level paraphyly and polyphyly: frequency, causes, and consequences, with insights from animal mitochondrial DNA. Ann. Rev. Ecol. Syst. 34, 397–423.
Hallatschek, O., Hersen, P., Ramanathan, S., Nelson, D.R., 2007. Genetic drift at expanding frontiers promotes gene segregation. Proc. Natl. Acad. Sci. USA 104, 19926–19930.
Harvey, J.B.J., Goff, L.J., 2006. A reassessment of species boundaries in *Cystoseira* and *Halidrys* (Phaeophyceae, Fucales) along the North American west coast. J. Phycol. 42, 707–720.
Hershkovitz, M.A., Lewis, L.A., 1996. Deep-level diagnostic value of the rDNA-ITS region. Mol. Biol. Evol. 13, 1276–1295.
Hoarau, G., Coyer, J.A., Veldsink, J.H., Stam, W.T., Olsen, J.L., 2007. Glacial refugia and recolonisation pathways in the brown seaweed *Fucus serratus*. Mol. Ecol. 16, 3606–3616.
Hormazabal, S., Shaffer, G., Leth, O., 2004. Coastal transitions zone off Chile. J. Geophys. Res. 109, 1–13.
Huelsenbeck, J.L., Ronquist, F., 2001. MRBAYES: Bayesian inference of phylogeny. Bioinformatics 17, 754–755.
Irwin, D.E., 2002. Phylogeographic breaks without geographic barriers to gene flow. Evolution 56, 2383–2394.
Kumar, S., Tamura, K., Nei, M., 2004. MEGA3: integrated software for Molecular Evolutionary Genetics Analysis and sequence alignment. Brief. Bioinform. 5, 150–163.
Knowles, L.L., 2004. The burgeoning field of statistical phylogeography. J. Evol. Biol. 17, 1–10.
Kuo, C.H., Avise, J.C., 2005. Phylogeographic breaks in low-dispersal species: the emergence of concordance among gene trees. Genetica 124, 179–186.
Lane, C.E., Lindstrom, S.C., Saunders, G.W., 2007. A molecular assessment of northeast Pacific *Alaria* species (Laminariales, Phaeophyceae) with reference to the utility of DNA barcoding. Mol. Phylogenet. Evol. 44, 634–648.
Lane, C.E., Mayes, C., Druehl, L.D., Saunders, G.W., 2006. A multi-gene molecular investigation of the kelp (Laminariales, Phaeophyceae) supports substantial taxonomic re-organization. J. Phycol. 42, 493–512.
Lünning, K., Müller, D.G., 1978. Chemical interaction in sexual reproduction of several Laminariales: release and attraction of spermatozoids. Z. Pflanzenphysiol. 89, 33–41.
Maggs, C.A., Castilho, R., Foltz, D., Hensler, C., Jolly, M.T., Kelly, J., Olsen, J.L., Perez, E., Stam, W.T., Vainola, R., Viard, F., Wares, J.P., 2008. Evaluating signatures of glacial refugia for North Alantic benthic marine taxa. Ecology 89, S108–S122.
Martínez, E.A., Cardenas, L., Pinto, R., 2003. Recovery and genetic diversity of the intertidal kelp *Lessonia nigrescens* (Phaeophyceae) 20 years after El Niño 1982/83. J. Phycol. 39, 504–508.
McCarthy, C., 1997. Chromas. Griffith University, Brisbane, Queensland.
Morse, G.E., Farrell, B.D., 2005. Interspecific phylogeography of the *Stator limbatus* species complex: the geographic context of speciation and specialization. Mol. Phylogenet. Evol. 36, 201–213.
Müller, K., 2006. Incorporating information from length-mutational events into phylogenetic analysis. Mol. Phylogenet. Evol. 38, 667–676.
Navarrete, S.A., Wieters, E.A., Broitman, B.R., Castilla, J.C., 2005. Scales of benthic–pelagic coupling and the intensity of species interactions: from recruitment limitation to top–down control. Proc. Natl. Acad. Sci. USA 102, 18046–18051.
Nei, M. (Ed.), 1987. Molecular Evolutionary Genetics. Columbia University Press, New York, NY, USA.
Omland, K.E., Baker, J.M., Peters, J.L., 2006. Genetic signature of intermediate divergence: population history of Old and New World Holarctic ravens (Corvus corax). Mol. Ecol. 15, 795–808.
Orita, M., Iwahana, H., Kanazawa, H., Hayashi, K., Sekiya, T., 1989. Detection of polymorphisms of human DNA by gel electrophoresis as single-strand conformation polymorphisms. Proc. Natl. Acad. Sci. USA 86, 2766–2770.
Ortlieb, I., Guzman, N., Marquardt, C., 2003. A longer-lasting and warmer interglacial episode during isotope MIS 11: marine terrace evidence in tropical western Americas. Earth's climate and orbital eccentricity: the marine isotope stage 11 questions. Geophys. Monogr. 137, 157–180.
Posada, D., Crandall, K.A., 1998. MODELTEST; testing the model of DNA substitution. Bioinformatics Application Note 14, 817–818.
Posada, D., Crandall, K.A., 2001. Intraspecific gene genealogies: trees grafting into networks. Trends Ecol. Evol. 16, 37–45.
Rogers, A.R., Harpending, H., 1992. Population growth makes waves in the distribution of pairwise genetic differences. Mol. Biol. Evol. 9, 552–569.
Rousset, F., 1997. Genetic differentiation and estimation of gene flow from *F*-statistics under isolation by distance. Genetics 145, 1219–1228.
Santelices, B., Meneses, I., 2000. A reassessment of the phytogeographic characterization of Temperate Pacific South America. Rev. Chil. Hist. Nat. 73, 605–614.
Schmitz, P., Cibois, A., Landry, B., 2006. Molecular phylogeny and dating of an insular endemic moth radiation inferred from mitochondrial and nuclear genes: the genus *Galagete* (Lepidoptera: Autostichidae) of the Galapagos Islands. Mol. Phylogenet. Evol. 45, 180–192.
Searles, R.B., 1978. The genus *Lessonia* Bory (Phaeophyta, Laminariales) in Southern Chile and Argentina. Br. Phycol. J. 13, 361–381.
Simmons, M.P., Ochoterena, H., 2000. Gaps as characters in sequence-based phylogenetic analyses. Syst. Biol. 49, 369–381.
Slatkin, M., 1993. Isolation by distance in equilibrium and non-equilibrium populations. Evolution 47, 263–279.
Sotka, E.E., Wares, J.P., Barth, J.A., Grosberg, R.K., Palumbi, S.R., 2004. Strong genetic clines and geographical variation in gene flow in the rocky intertidal barnacle *Balanus glandulata*. Mol. Ecol. 13, 2143–2156.
Sunnucks, P., Wilson, A.C.C., Beheregaray, L.B., Zenger, K., French, J., Taylor, A.C., 2000. SSCP is not so difficult: the application and utility of single-stranded conformation polymorphism in evolutionary biology and in molecular ecology. Mol. Ecol. 9, 1699–1710.
Swofford, D.L., 2002. PAUP*. Phylogenetic Analysis Using Parsimony (* and other methods). Version 4, Sunderland, Massachusetts.
Thiel, M., Macaya, E.C., Acuña, E., Arntz, W.E., Bastias, H., Brokordt, K., Camus, P.A., Castilla, J.C., Castro, L.R., Cortés, M., Dumont, C.P., Escribano, R., Fernandez, M., Gajardo, J.A., Gaymer, C.F., Gomez, I., González, A.E., González, H.E., Haye, P.A., Illanes, J.E., Iriarte, J.L., Lancellotti, D.A., Luna-Jorquera, G., Luxoro, C., Manriquez, P.H., Marín, V., Muñoz, P., Navarrete, S.A., Perez, E., Poulin, E., Sellanes, J., Sepúlveda, H.H., Stotz, W., Tala, F., Thomas, A., Vargas, C.A., Vasquez, J., Vega, J.M.A., 2007. The Humboldt Current System of northern and central Chile. Oceanogr. Mar. Biol. Annu. Rev. 45, 195–344.
Vásquez, J.A., 2008. Fate of Chilean Kelps: re-sources for a sustainable fishery. J. Appl. Phycol. 20, 457–467.
Vanderpoorten, A., Long, D.G., 2006. Budding speciation and neotropical origin of the Azorean endemic livewort, *Leptoscypus azoricus*. Mol. Phylogenet. Evol. 40, 73–83.
Voisin, M., Engel, C.R., Viard, F., 2005. Differential shuffling of native genetic diversity across introduced regions in a brown alga: aquaculture vs. maritime traffic effects. Proc. Natl. Acad. Sci. USA 102, 5432–5437.
von der Heyden, S., Prochazka, K., Bowie, R.C.K., 2008. Significant population structure and asymmetric gene flow patterns amidst expanding populations of *Clinus cottoides* (Perciformes, Clinidae): application of molecular data to marine conservation planning in South Africa. Mol. Ecol. 17, 4812–4826.

Wares, J.P., Gaines, S.D., Cunningham, C.W., 2001. A comparative study of asymmetric migration events across a marine biogeographic boundary. Evolution 55, 295–306.

Yoon, H.S., Boo, S.M., 1999. Phylogeny of Alariaceae (Phaeophyta) with special references to *Undaria* based on sequences of the RuBisCo spacer region. Hydrobiologia 398 (399), 47–55.

Yoon, H.S., Lee, J.Y., Boo, S.M., Bhattacharya, D., 2001. Phylogeny of Alariaceae, Laminariaceae, and Lessoniaceae (Phaeophyceae) based on plastid-encoded RuBisCo spacer and nuclear-encoded ITS sequence comparisons. Mol. Phylogenet. Evol. 21, 231–243.

Yotsukura, N., Denboh, T., Motomura, T., Horiguchi, T., Coleman, A.M., Ichimura, T., 1999. Little divergence in ribosomal DNA internal transcribed spacer -1 and -2 sequences among non-digitate species of *Laminaria* (Phaoephyceae) from Hokkaido. Japan Phycol. Res. 47, 71–80.